




Use of phosphorylated chitosan/alumina nanoadditives for polymer performance improvement

Mehdi Hatami · Nima Rahnama · Hassan Karimi-Maleh ·
Nader Djafarzadeh · Mohammad Qandalee · Reza Setva · Fatemeh Karimi ·
Carlos J. Durán-Valle  · Ignacio M. López-Coca · Alireza Sharifi

Received: 23 November 2021 / Accepted: 4 June 2022 / Published online: 22 June 2022
© The Author(s) 2022

Abstract In this research, a new generation of ternary nanocomposites based on poly(ethylene terephthalate) (PET), phosphorylated chitosan and surface modified alumina nanoparticles were fabricated in four steps. The phosphorylation process was targeted for the insertion of phosphorus moieties as a flame retardant agent in the final PET nanocomposite. Likewise, environmentally friendly nano-alumina was used for PET matrix to improve the thermal properties of PET in collaboration with organic anchored phosphorus moieties. Alternatively, the presence of bio-safe modified alumina nanoparticles in combination with phosphorylated chitosan simultaneously improved the antibacterial activity and thermal properties of the PET matrix. Furthermore, the

effects of the phosphorylated chitosan and alumina nanoparticles on the morphology and thermal properties of nanocomposites were inspected by different approaches. The structure and distribution of the nanoscale particles in PET were analyzed by scanning electron microscopy. In addition, differential scanning calorimetry and thermogravimetric analyses were used for the in-depth evaluation of the thermal properties of prepared nanocomposites. Prepared nanocomposites showed better growth inhibition activities against *Escherichia coli* bacteria compared to the PET and PET/phosphorylated chitosan samples. Also, the thermal characteristics of prepared nanocomposites were considerably improved.

M. Hatami
Polymer Research Laboratory, Department of Polymer
Science and Engineering, University of Bonab, P.O.
Box 5551761167, Bonab, Iran

N. Rahnama
Entekhab Petrochemical Company, Asaluyeh, Bushehr,
Iran

H. Karimi-Maleh · F. Karimi
School of Resources and Environment, University
of Electronic Science and Technology of China,
Xiyuan Ave, P.O. Box 611731, Chengdu,
People's Republic of China

N. Djafarzadeh
Department of Chemistry, Miyaneh branch, Islamic Azad
University, Miyaneh, Iran

M. Qandalee
Department of Basic Sciences, Garmsar Branch, Islamic
Azad University, Garmsar, Iran

R. Setva · A. Sharifi
Department of Polymer Engineering, Mahshahr Branch,
Islamic Azad University, Mahshahr, Iran

C. J. Durán-Valle (✉)
Facultad de Ciencias, IACYS, Universidad de
Extremadura, 06006 Badajoz, Spain
e-mail: carlosdv@unex.es

I. M. López-Coca
Escuela Politécnica, INTERRA, Universidad de
Extremadura, 10003 Cáceres, Spain

Keywords Antibacterial properties · Alumina · Chitosan · Nanocomposite

Introduction

Poly(ethylene terephthalate) (PET) is an important macromolecule widely used in different industries, especially in the manufacture of barriers, fibers, sheets and films. PET has outstanding physical, mechanical and chemical features and belongs to the polyester category in polymer chemistry. The attractiveness of PET is related to the various favorable properties of the polyester family, including low moisture regain, suitable strength, respectable heat and dimensional stability, and lower production costs compared to other polymers (Visakh and Liang 2015). Many additives were used in the processing of PET to improve the final properties of this polymer. This fact is mainly related to the limited reaction sites of PET. Recently, with the development of nanotechnology in polymer industries, in order to improve the characteristic features of PET, some nanoscale additives have been used in PET grade products (Visakh and Liang 2015; Barber 2017; Madakbas et al. 2017). Biopolymers such as chitin, chitosan, and cellulose play important roles in increasing the biocompatibility of composite materials. The use of novel biocomposites has drastically increased for the benefit of the protection of the environment. The development of chitosan applications as a low-cost material that was prepared in shrimp industries is a new strategy for improving the degradation of synthetic polymers in the environment. Therefore, chitosan has become popular in many categories due to its uncommon biological, mechanical, chemical, and physical properties (Zhang et al. 2020; Jia et al. 2016; Phung and Sugimoto 2018). Conversely, some difficulties have appeared in the application of chitosan due to the low solubility of this biopolymer in common solvents. One of the promising approaches in this category is related to the chemical treatment of chitosan to insert new functional units in the structure of this biopolymer (Jothimani et al. 2017). The chemical modification of chitosan is interesting, since these modifications would not alter its skeleton. These modifications have been shown to keep the unique physicochemical and biochemical properties of chitosan (Khoee et al. 2017). Chitosan is a linear polysaccharide comprised

of β -(1–4)-linked D-glucosamine and N-acetyl-D-glucosamine (Chaudhary et al. 2020). Nowadays, due to the increasing demands for bio-based polymers, the application of different derivatives of modified biopolymers (MBPs) is greater than before. One of the new categories of MBPs is the nanocomposites based on blends of MBPs matrices with commercially available polymers (Chaudhary et al. 2020; Naffakh et al. 2014; Hassan et al. 2014; Al et al. 2017). Hybrid MBPs have attracted great interest, as the insertion of inorganic segmented polymer guests in main polymer hosts can improve the properties of complex matrices (Becerra et al. 2020; de Oliveira et al. 2019; dos Santos et al. 2014; Ghanbari and Gharufi 2002; Melo et al. 2017; Monteiro et al. 2019; Siva et al. 2022; Subashini et al. 2022). The extraordinary properties of hybrid MBPs are a vital requirement for innovative composites of high-performance materials (Yin et al. 2019; de Moura et al. 2012; Mallakpour and Motirasoul 2017). Insertion of inorganic enriched MBPs into other polymer matrices can enhance the mechanical, thermal, and optical properties of composite macromolecules (Dufresne et al. 2013; Rodriguez et al. 2016; Hatami 2018). Therefore, the prepared biocomposites display the triple properties of guest biopolymer, nanoscale filler and hosted matrix. The subsequent properties of the obtained materials are better than those of all used ingredients. The demand for biocompatible compounds of PET has increased recently (Joo et al. 2018; Sadhasivam et al. 2018; Fidanovski et al. 2018). Also in recent years, numerous nanosized constituents have been used to improve the performance of PET matrices (Dubrovsky et al. 2018; Rathod et al. 2017; Jung et al. 2018). For example, De Filipo et al. (2006) reported the preparation of a flexible nano-photo-electrochromic PET-TiO₂-PO₄-MB by deposition of the nanocrystalline TiO₂ layer on conductive PET. The photo-electrochromic properties were created based on the covalent chemical bonds of methylene blue (MB) on the TiO₂ film in a one-step process. The results obtained by this research group show that the film undergoes quick discoloration due to the oxidization reaction of MB. Wang et al. (2018) reported the preparation of a new generation of BiOI/SnO₂/PET nanocomposites by using successive ionic layer adsorption reaction (SILAR), and a hydrothermal method. This research group used this polymer material as a carrier of a photo-catalyst to support the BiOI/SnO₂ nanostructure. Experimental results by

Wang's research group indicated that PET/BiOI/SnO₂ displayed excellent photo-catalytic capability towards methyl orange (MO) and tetracycline (TC) under visible light irradiation. Jalali et al. (2017) reported the fabrication and characterization of the new magnetite nanocomposite based on Co_{0.7}Zn_{0.3}Fe₂O₄/poly(ethyleneterephthalate)/silver ingredients. This material was designed to improve the antimicrobial activity against Gram-negative and Gram-positive bacteria. They prepared the nanocomposite in a two-step procedure. At the first step, Co_{0.7}Zn_{0.3}Fe₂O₄ nanoparticles were fabricated and then covered by the PET polymer. At the second step, Ag nanoparticles were decorated on the surface of the PET shell to obtain the metallic-polymer alloy-type nanocomposites. Results obtained by this research team confirmed that these nanocomposites have excellent potential in environmental remediation applications.

In continuation of our efforts in the design and production of innovative polymeric compounds (Mehdipour-Ataei and Hatami 2007; Hatami et al. 2020, 2022; Mehdipour-Ataei et al. 2009), we targeted the fabrication of phosphorylated chitosan/modified alumina nano-additives for a unique PET polymer matrix. Based on the experimental experiences in the preparation of nanocomposites, the hanging over of the inorganic nanostructure by in-situ chemical process on second polymeric media could improve the chemical and physical properties of final nanocomposites due to the good dispersion of nanostructures in the final matrix. In our previous study (Hatami et al. 2022), the fabrication of PET/phosphorylated chitosan/silver nanocomposites was achieved. Due to the simultaneous good antibacterial and thermal properties of prepared nanocomposites, in this study the authors decided to change the nanostructure in additive formulation to compare the novel nanocomposites with the previous one. Based on the unique properties of the nanoscale alumina nanoparticles such as antibacterial and thermal stability properties, these nanoparticles were selected for this study and the results were compared with previous publications (Table 1). The combination of alumina nanofillers and chitosan biopolymers brings suitable features for the properties of a new generation of PET bionanocomposites. Based on our experiences in the production of hybrid composites (Hatami and Yazdan Panah 2017; Hatami et al. 2015; Hatami 2017; Ahmadi et al. 2018; Yousefi et al. 2019) for diverse applications,

the novel PET/alumina/phosphorylated chitosan bionanocomposites could be candidate for application in the food packaging industry.

Many additives have historically been used for PET polymer modification. The insertion of additives in PET structure improves the processability, and durability along with a better performance of the polymer in final application areas. In recent years, nanostructure additives are keeping their own position in the PET industry. Some companies like NYACOL, and BYK offer powders, colloidal dispersions, and polymeric structures as masterbatches for use as PET additives in the production of films, fibers and bottles. These commercial additives were formulated according to the desired characteristics of a product. These additives are added in the polymerization step or during the processing of PET resin. Some of these additives have different functionalities. Different nanostructure materials were illustrated as PET additives. Some of these additives were presented in Table 1. As shown in this Table, suppliers provide carriers for the insertion of nanostructures in polymeric media. But in most cases, the colloidal and polymer-supported structures are preferred due to the good distribution and prevention of agglomeration of the nanostructures in the final media.

In the present article, we report the manufacture of surface-modified aluminum oxide nanoparticles stabilized on phosphorylated chitosan in PET matrix by physical and chemical interactions. The four main advantages could be assigned to this strategy. (1) The synergistic effects of properties in the modified formulation based on chitosan and nano-alumina in antibacterial properties (organic antibacterial material in collaboration with inorganic structure). (2) Bearing the inorganic phosphor in organic media by phosphorylation of chitosan (modification of organic chitosan biopolymer with phosphor moieties). (3) Improvements in the thermal properties of the final product by the collaboration of properties of phosphor and nano-alumina (due to their intrinsic properties of them). (4) Fabrication of polymer nanocomposite in the best state (without aggregation or agglomeration of nanoparticles in nanocomposite and good blending of chitosan and matrix) and with excellent designed application properties. The fabrication of the Al₂O₃/phosphorylated chitosan/PET bionanocomposite was performed in four steps. Firstly, the chitosan was modified by a phosphorylation reaction. In the

Table 1 Results of previous publications

Nano-additive structure	Particle size	Carrier	Application	References
Antimony tin oxide	50–90 nm	Ethylene glycol	This additive provides excellent reheat characteristics in PET bottle resin and outstanding IR absorption in films and fibers	https://www.nyacol.com/
Silica nanoparticles (SiO ₂)	20–120 nm	Ethylene glycol	Nanoscale SiO ₂ provides improved abrasion resistance and anti-blocking properties for PET film	https://www.nyacol.com/
Titania nanoparticles (TiO ₂)	30 nm	Ethylene glycol	Nanoscale titanium dioxide provides UV absorbing properties	https://www.nyacol.com/
indium tin oxide (ITO)	64 nm	Ethylene glycol	ITO nanostructure is useful for infrared reflective coatings, antistatic coatings and solar cells	https://www.nyacol.com/
Silver	< 100 nm	Doped carbon black	Nanosilver doped CB provides antibacterial properties	De Guzman et al. (2021)
Layered double hydroxide	80–100 nm	Sulfanilic acid solution in water	LDH provided reflection properties of the UV Light	Ou et al. (2004)
Silver	50–60 nm	Phosphorylated chitosan (PC)	Silver loaded PC provides flame retardant and antibacterial properties	Hatami et al. (2022)
Silver	< 100 nm	Reduced graphene oxide(rGO)	Silver loaded rGO enhances UV-protective of textile	Babaahmadi et al. (2022)
Graphene	Thickness 2 nm	Trimellitic anhydride	Graphene improves the mechanical properties of samples	Aoyama et al. (2018)
Antimony-doped tin oxide	20 nm	Ethylene glycol	Kinetic investigations were achieved	Chen et al. (2008)
Al ₂ O ₃	10 nm	Ethylene glycol	Slightly changes the melting temperature	Lim et al. (2013)
Silver	< 100 nm	Immobilized in silica	Antimicrobial filaments	Guerra et al. (2018)
TiO ₂ nanoflowers	< 200 nm	In situ preparation	Exhibits good self-cleaning performance	Peng et al. (2012)
Organo modified Silica	30 nm	Ethylene glycol	The addition of nanoparticles increases the crystallizing temperature and melting point of the polymer	Liu et al. (2004)
Mixed TiO ₂ , SiO ₂ , and ZnO	< 100 nm	Powdered form	Increases the UV-blocking effects	Bahramian, (2021)
Aluminium Nano Platelets (AP)	Less than 45 μm	Powdered form	AP improves the mechanical properties of nanostructures	Anis et al. (2022)
Montmorillonite Cloisite 20A	Less than 10 μm	Powdered form	MMTs improve the physical and barrier properties in thermoplastic compounds	Lima et al. (2021), Scheirs and Long, (2004); https://www.byk.com

second step, the sonochemical assisted production method was used for the surface treatment of Al_2O_3 nanoparticles by Leucine amino acid moieties. In the third step, the surface-treated Al_2O_3 nanostructures were dispersed in phosphorylated chitosan by the solution mixing method. Finally, Al_2O_3 /phosphorylated chitosan/PET bionanocomposites were fabricated by the well-known melt mixing method. The benefit of this four-step procedure is that the surface-adapted nanoparticles in combination with modified biopolymer are stabilized by functional units of the PET matrix. Therefore, the PET antibacterial property was improved using the combined characteristics of the nanoparticles and chitosan. Moreover, the thermal properties of the obtained nanocomposites were enhanced due to the presence of elemental phosphorous, in addition to alumina as metal oxide nanoparticles, in the structure of the polymer matrix nanocomposites.

Experimental

Materials

In this research, polyethylene terephthalate (PARS PET-BG781) was obtained from Shahid Tondgoyan Petrochemical Company (Iran) and was used as received. The specification of used PET was reported at reference (Hatami et al. 2022). Chitosan biopolymer (91.8% degree of deacetylation) was provided by Sigma-Aldrich. Acetic acid, DMF, urea, and ortho-cresol were purchased from Merck Chemical Co. Nano aluminum oxide (Al_2O_3) powder was acquired from Neutrino Co. with average particle sizes of 18–25 nm. Orthophosphoric acid (H_3PO_4) was supplied by Sigma-Aldrich. All reagents were used as received without any purification.

Characterizations and instruments

The FT-IR spectra were obtained using a Spectrum GX (Perkin Elmer, USA). Spectra were recorded between 4000 and 400 cm^{-1} with a resolution of 2 cm^{-1} . The TGA measurements were performed using a TGA 4000 model (Perkin Elmer). The sample was heated in a platinum pan with 60.0 mL/min nitrogen at 10 $^\circ\text{C}/\text{min}$ at 600 $^\circ\text{C}$. The sample weighed approximately 10 mg. The thermal properties of

samples were studied by differential scanning calorimetry (DSC; Metler Toledo). A sample of about 5 mg from each composition was scanned in a cycle of heating–cooling–heating from 30 to 300 $^\circ\text{C}$ at 10 $^\circ\text{C min}^{-1}$ in aluminum pans. The samples were kept at 300 $^\circ\text{C}$ for 5 min to erase any previous thermal history. The DSC apparatus was purged with N_2 gas at a rate of 50 mL min^{-1} . The glass transition temperature was determined from the second heating scan, as the first scan was conducted to remove the thermal history. A scanning electron microscope (SEM; KYKY microscope Model EM3200, accelerating voltage 26 kV, Japan) was used to study the morphology of the fractured surfaces. Before performing the tests, the samples were cryofractured in liquid nitrogen. Then, the fracture surface was coated with gold and observed by SEM. Intrinsic viscosity (IV) is defined as the reduced viscosity or inherent viscosity at zero concentration for a polymer solution. The intrinsic viscosity measurements were carried out according to ASTM-D 4603, using dichloroacetic acid as a solvent. IV was examined using an automatic Ubbelohde capillary type viscometer. The intrinsic viscosity measurement system includes a capillary viscometer, Type II, and a water bath at a constant temperature of 25 ± 0.02 $^\circ\text{C}$. Initially, different concentrations (1–10 g L^{-1}) of polyethylene terephthalate were dissolved in dichloroacetic acid solvent at 230 $^\circ\text{C}$. Right before loading the solution into the viscometer, the solution was filtered using a 0.45-micron sized hydrophilic membrane filter. The IV and relative viscosity (η_{rel}) of the samples were calculated. Ultimately, the intrinsic viscosity was calculated for each sample. Potentiometric titration, a method for evaluating the potential changes of the solvent, was used to determine the concentration of carboxylic end groups according to ASTM D 7409–07. The polymer sample was dissolved in a mixture of ortho-cresol and chloroform (at a weight ratio of 70 to 30) under reflux conditions at 80 $^\circ\text{C}$. After cooling the solution to room temperature in the cold-water bath, the concentration of the carboxylic end groups was determined by titration with an ethanolic potassium hydroxide solution (0.05 M). The potentiometric titrator (Metrohm Switzerland Company) was used with Tiamo software to calculate the concentration of carboxylic end groups. A colorimetric test was performed for PET and its nanocomposites in accordance with ASTM D6290-5 using a colorimeter

(ColorFlex®, Hunterlab, USA) at a viewing angle of 10 degrees. This instrument provided L^* , a^* and b^* values, where L^* is the lightness component ranging from 0 (black) to 100 (white), and parameters a^* (from greenness to redness), and b^* (blueness to yellowness) are the two chromatic components. The PET sheets were sterilized in an autoclave and cut to sizes of $2 \times 2 \text{ cm}^2$. Concentrations of 5, 10, 20 and 40 mg mL^{-1} of sterilized medium were used. The bacterial culture in this stage was Muller Rintonbroyh, from Glab Company. The samples were placed in test tubes containing 4 mL of culture medium. The test tubes were then placed in an autoclave at $121 \text{ }^\circ\text{C}$ and 15 psi pressure for 15 min. After sterilization, the tubes were placed in the laboratory to cool down and then *E. coli* was added to the test tubes. *E. coli* was cultured in a nutrient broth for 24 h in an incubator. After reaching turbidity, $100 \text{ }\mu\text{L}$ of the culture was added to each of the test tubes. After incubation at $37 \text{ }^\circ\text{C}$ for 24 h, the resulting bacterial colonies in the plates were counted using sample light absorption at the desired wavelength (580–600 nm). The bacterial growth parameter was measured using the difference between the numbers of colonies of bacteria with samples and those of bacteria in the blank vials. The PET/phosphorylated chitosan/nano alumina bionanocomposites with different wt/wt percentages were prepared using a Brabender internal mixer (Germany) with a volume of 350 cm^3 and a speed of 60 rpm at $260 \text{ }^\circ\text{C}$ for 8 min.

Chitosan phosphorylation

The phosphorylation process of chitosan was achieved according to the reference (Hatami et al. 2022). The solutions of 0.03275 M chitosan, 1.075 M of orthophosphoric acid, and 8.325 M of urea in DMF were prepared. The total 200 mL of the mixture was stirred at $150 \text{ }^\circ\text{C}$ for an hour. After cooling, the solid sample was filtered. The product was washed with deionized water. The amount of chitosan phosphate obtained was 18.3 g. The phosphorous content in phosphorylated chitosan was 5.8%.

Surface modification of Al_2O_3 nanoparticles

Alumina nanostructures were dried at $110 \text{ }^\circ\text{C}$ in an oven for 24 h to remove the adsorbed water. The dried nano aluminum oxide (0.2 g) was sonicated

for 15 min. in absolute ethanol, and then 15% (w/w) Leucine amino acid (Luc) to nano Al_2O_3 was added to the mixture and sonicated for 20 min. The brown precipitate was separated and dried at $60 \text{ }^\circ\text{C}$ for more than 24 h.

Fabrication of stabilized nano Al_2O_3 onto the phosphorylated chitosan

Phosphorylated chitosan powder, 10% (W/V), was dissolved in a 0.5 M acetic acid solution at $65 \text{ }^\circ\text{C}$ to give a clear solution (about 12 h). Proper amounts of surface-modified nano alumina were dispersed in 20 mL 0.5 M acetic acid solution. A uniform colloidal dispersion was obtained after sonication for 15 min at room temperature. In the next step, the required phosphorylated chitosan solution was mixed with modified Al_2O_3 nanoparticles. The samples obtained were sonicated for 4 h. After sonication, the solvent was removed and the obtained solid washed twice with ethanol, and then dried in a vacuum at $85 \text{ }^\circ\text{C}$ for 2 h.

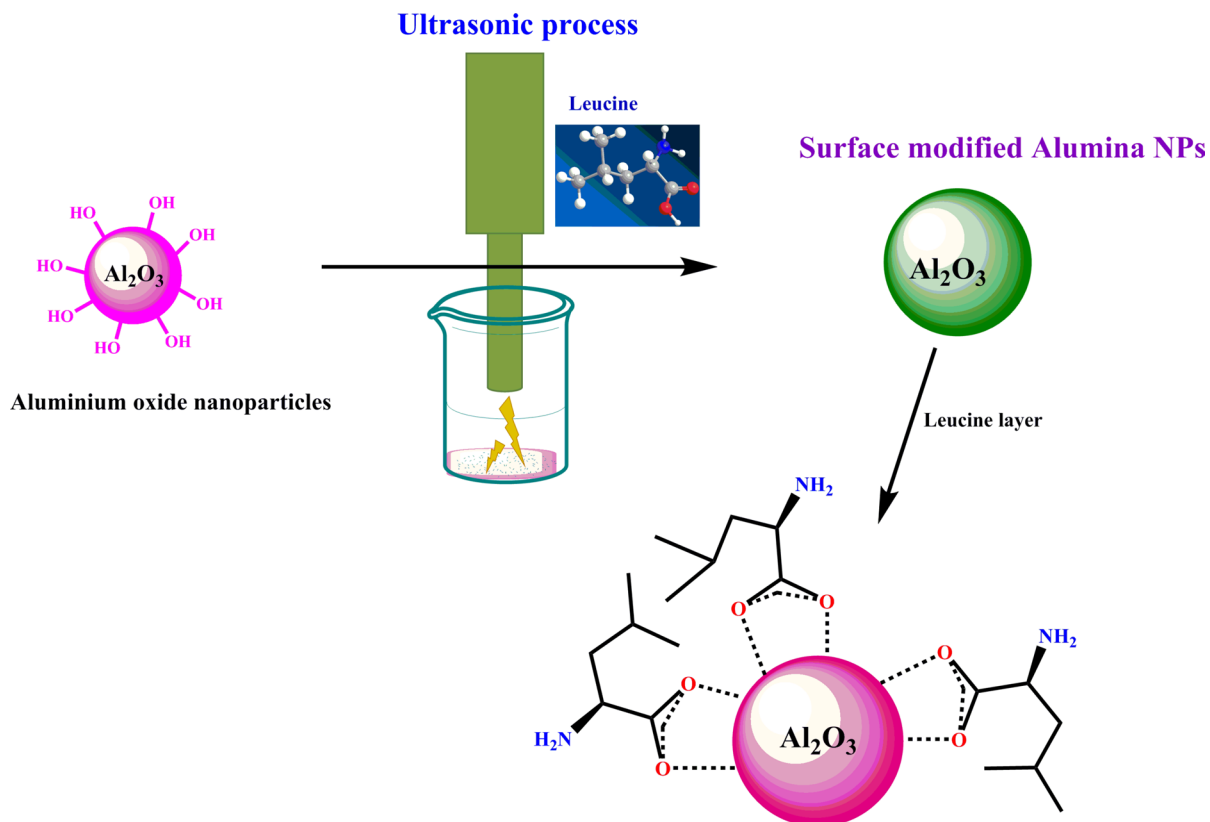
Bionanocomposite preparation route

The nanocomposites with four and six weight/weight percent were fabricated by Brabender internal mixer with a speed of 60 rpm and a volume of 350 cm^3 at $260 \text{ }^\circ\text{C}$ for eight minutes. The choice of 4–6wt% of fillers was followed by the previous study (Hatami et al. 2022). The resulting blend was well mixed. After preparation, the obtained solid was washed twice with water and then dried in a vacuum at $85 \text{ }^\circ\text{C}$ for 2 h. Afterward, the provided samples were subjected to a compression molding procedure. The samples were provided in the sheet form with the assistance of hydraulic presses under a pressure of 10 mega Pascal in the dimensions of $0.3 \times 10 \times 10 \text{ cm}^3$ at $260 \text{ }^\circ\text{C}$.

Results and discussion

Surface modification of alumina nanoparticles by ultrasonication process

We applied the surface modification method for insertion of organic functional units on the exterior surface of alumina nanoparticles. Alpha-amino acids were investigated as surface coating materials



Scheme 1 Surface modification of alumina nanoparticles by ultrasonication process

to modify the surface of inorganic nanoparticles; indeed, the carboxylic acid functional unit of α -amino acids could be applied to the surface of alumina nanoparticles. Among the different amino acids, Leucine (Leu) attracts great interest, since it is an essential amino acid and displays pharmacological action in humans; moreover, it has also been proved to promote protein biosynthesis via the phosphorylation reaction. Scheme 1 graphically shows that the hydroxyl units of the surface of Al_2O_3 nanoparticles are needed to physically attach to the carboxylic group of leucine. The alumina nanoparticles external surface is changed by physical van der Waals forces. The O–H stretching in the FT-IR spectrum related to the hydroxyl unit on the surface of alumina nanoparticles disappeared after surface modification. The illustration of the preparation of a thin film of leucine on the surface of alumina is shown in Scheme 1. The ultrasonic irradiation helped to remove the accumulation of alumina nanoparticles. This method has been previously

described elsewhere (Hatami and Yazdan Panah 2017; Hatami et al. 2015; Hatami 2017).

FT-IR inspection of surface modified alumina nanoparticles

FT-IR spectra of the pure Al_2O_3 and the surface-treated Al_2O_3 with amino acid modifier are displayed in Fig. 1. In the FT-IR spectrum of nanoscale Al_2O_3 , two distinctive peaks were detected at 3528 and 1587 cm^{-1} (Fig. 1a). The wide band at 3528–3267 cm^{-1} can be assigned to the vibration of the hydroxyl units of adsorbed water by the alumina nanoparticles. The sharp band at around 1600 cm^{-1} can be attributed to the bending vibrations of H–O units on the exterior of Al_2O_3 nanoparticles. The band at 550 cm^{-1} was related to the Al–O. The spectrum of the surface-modified alumina is shown in Fig. 1b. The feeble stretching band of the O–H groups was observed at 3285 cm^{-1} and demonstrates the success of the surface modification process of the alumina

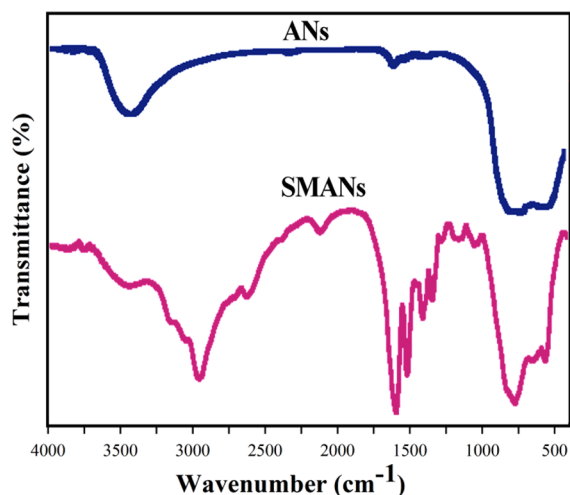
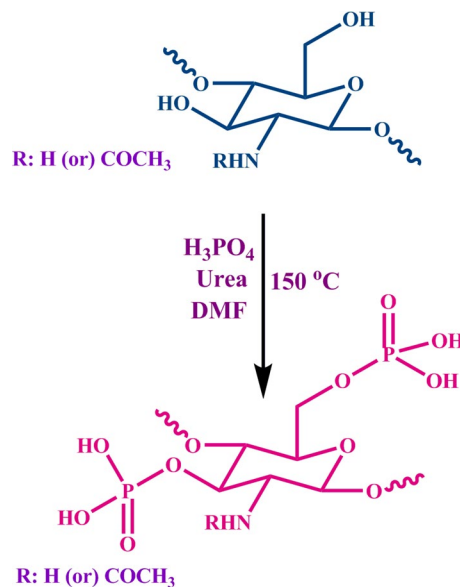


Fig. 1 FT-IR spectra of (top) pure Al_2O_3 nanoparticles, (bottom) the surface modified Al_2O_3 with amino acid modifier

nanoparticles after ultrasonication. The peak at 3450 cm^{-1} (Fig. 1b) was associated with the amino functional unit on the surface of alumina after modification. After modification, the distinctive band of the aliphatic unit of the amino acid appeared in the spectrum of surface modified nanoparticles. Furthermore, the vibrations of the $-\text{OH}$ units on the surface of alumina were reduced; however, due to the presence of amine functional units on the structure of the modified alumina, the vibration intensities in the range of $3400\text{--}3200\text{ cm}^{-1}$ were not reduced. This fact was mirrored by the ability of amine bonds to create hydrogen bonds. These results indicate that the amino acid moieties were attached to the surface of the alumina nanoparticles.

Fabrication of innovative antibacterial/thermally stable PET bionanocomposites

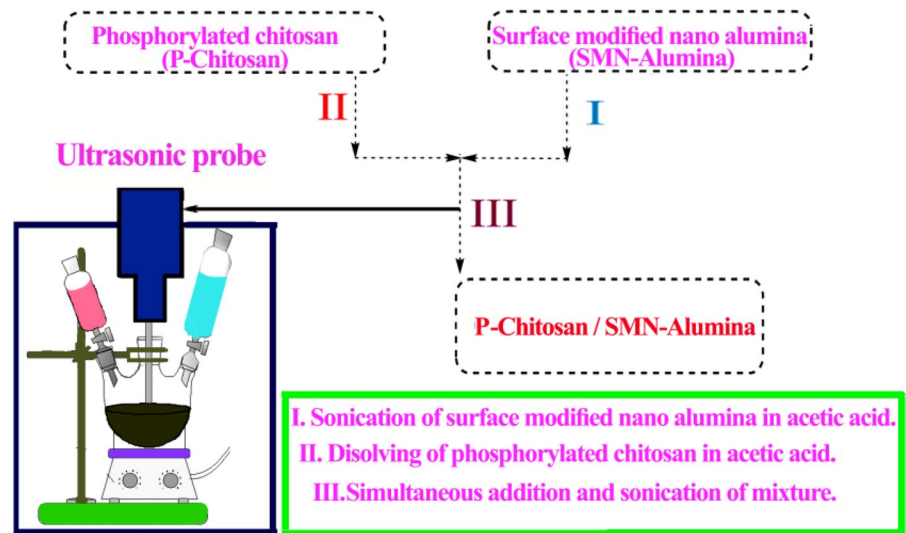
The capabilities developed by the Hatami group in the manufacture and characterization of novel multifunctional bionanocomposites led to the exploration of interesting areas of applicability for PET. In this project, we aimed at the simultaneous development of antibacterial and flame retardant properties in PET, which is a widely commercially accessible polymer. The description of similar products to the PET employed in this study is presented in Table 1. Many flame-retardant compounds have been used in the industry to control the fire-related properties of



Scheme 2 Preparation of phosphorylated chitosan

final products. These materials are classified based on chemical composition and physical properties. In general, flame retardants are categorized based on whether they contain bromine, chlorine, boron, nitrogen, phosphorus or metals (Ahmadi et al. 2018). On the other hand, diverse antibacterial compounds are known, although chitosan biopolymer and alumina nanoparticles are less popular among them. Therefore, to link the good properties of these two categories of organic and inorganic materials to antibacterial and flame retardant properties, phosphorylated chitosan and alumina nanoparticles were chosen as building blocks for this study. Phosphorous and aluminum oxide were selected for their flame retardant properties, and the chitosan skeleton and aluminum oxide were also carefully chosen as antibacterial agents. Therefore, to achieve the goal of the project, chitosan was phosphorylated and supported onto alumina nanoparticles. The application of this strategy allowed us to obtain PET bionanocomposites with unusual dual properties. The flame retardant building blocks containing phosphorus were obtained in a single step by means of a phosphorylation reaction, carried out by immersing chitosan in a solution of urea and orthophosphoric acid in DMF; this procedure is illustrated in Scheme 2. Subsequently, the phosphorylated chitosan was deposited on the alumina nanoparticles

Scheme 3 Insertion of alumina nanoparticles into the phosphorylated chitosan



by the ultrasound method. This process is illustrated in Scheme 3.

Finally, the bionanocomposites were prepared using the melt-mixing procedure of PET and the chitosan-derived nanocomposite. This method is shown in Scheme 4.

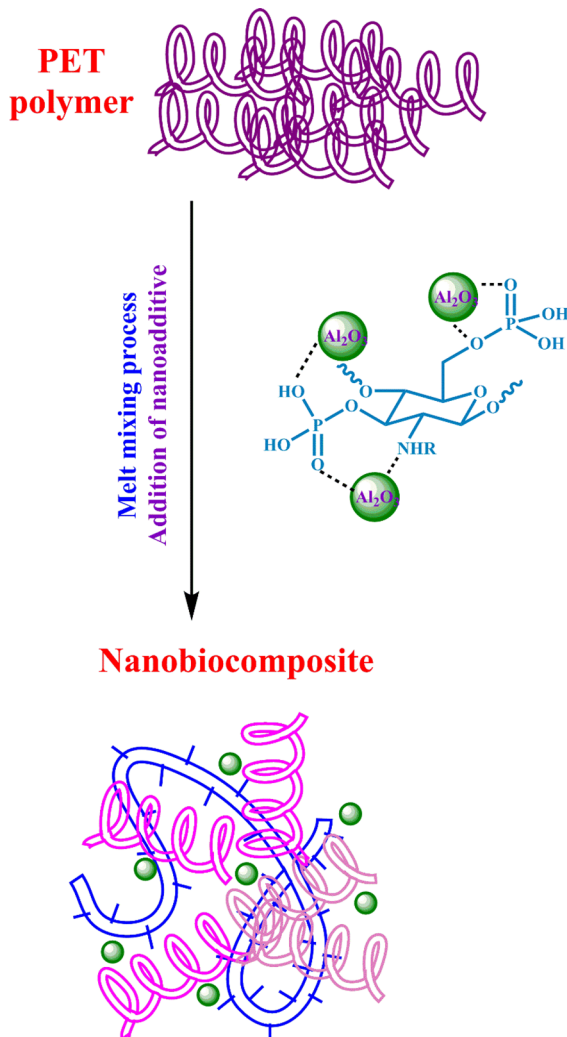
FT-IR characterizations of PET/phosphorylated chitosan/alumina bionanocomposites

The chemical structures of the pure PET matrix and the derived bionanocomposites were characterized based on chemical functional units by FT-IR analysis. The spectra registered for PET and samples containing various concentrations of phosphorylated chitosan/nano alumina are shown in Fig. 2. Characteristic peaks for PET have the following wavenumbers: 3431 cm^{-1} , 2970 cm^{-1} , 1732 cm^{-1} , 1246 cm^{-1} , and 1083 cm^{-1} , corresponding to the hydroxyl (-OH), methyl (-CH₃), carbonyl (C=O), methylene (-CH₂-) and ether (C-O-C) groups, respectively. The characteristic peaks of phosphorylated chitosan appear at 1240 and 1450 cm^{-1} , corresponding to the asymmetric stretching of the P=O bond. The appearance of peaks at 1343 , 1260 , 1020 , 974 and 850 cm^{-1} can be attributed to the presence of alumina nanoparticles in the nanocomposites; increasing the concentration of Al₂O₃ in the nanocomposites also increased the intensity of these peaks. These spectra show the existence of promising interactions between PET,

phosphorylated chitosan, and surface-modified alumina nanoparticles.

TGA investigations of polymer and bionanocomposites

The thermal stabilization of polymers is one of the main strategies for improving the quality of polymer processing. In this regard, the insertion of different modified structures such as hindered phenols, alkyl aryl amines, and different polymeric structures have been reported. On the other hand, inorganic structures also beside the organic molecules were used in industries. The combination of the organic molecule with an inorganic segment in the one structural unit is a fascinating idea. Therefore, the new synthesis procedures could be helped for obviation of industrial demands. The presence of organic-inorganic nanoscale components in polymer matrices improves the thermal stability of matrices. Therefore, the thermal stability of prepared polymer modified nanostructures is one of the most important usage criteria for different applications. The stability of polymer-modified its wide application in synthesis processes which nowadays are in great demand from the point of view of industrial. PET belongs to the polyester family. Besides many advantages of PET, some weak points are presented in the structure that may affect the performance of this polymer in the final application area. The sensitivity of polyesters to the hydrolysis process is one of the weak points of these



Scheme 4 Illustration of the fabrication procedure for PET bionanocomposites

polymers. Therefore the use of new strategies such as modification of polymer to overcome the weakness of matrix creates new innovative visions in this area. Thermogravimetric analysis (TGA) is a useful analytical instrument that can be used to evaluate the mass loss or mass gain of a solid as a function of temperature (Yousefi et al. 2019). In this research, the thermal durability of polymers and polymer-based bionanocomposites was analyzed using this technique. With this method, it was possible to measure the thermal characteristics of the samples, such as the initial decomposition temperature, maximum decomposition temperature, the degradation rate of the samples,

the char yield (CY) of the material at the evaluated temperature and limiting oxygen index (LOI). The stability of polymer modified its wide application in synthesis processes which nowadays are in a great demand from the point of view of industrial. Figure 3 shows the sample TGA, DTG and DTA analysis results for bionanocomposite 4 wt%. The comparative TGA thermograms of neat PET, PET/phosphorylated chitosan and bionanocomposites are illustrated in Fig. 4. The data of the TGA analysis results are presented in Table 2. The LOI values for the macromolecule and related bionanocomposites were calculated based on the Van Krevelen equation (Van Krevelen and Hoftzyer 1976), and the results are also presented in Table 2. The increase of char yield values of bionanocomposites and increments in the LOI values indicated that the thermal stability of bionanocomposites was gradually enhanced. Consequently, the thermal stability of these PET derivatives was improved by simultaneous application of phosphorylated chitosan and modified nanoscale alumina. The qualified DTG thermograms of neat PET, PET/phosphorylated chitosan and obtained composites are shown in Fig. 5.

Differential scanning calorimetric investigations

The glass transition temperature (T_g), melting temperature (T_m), and crystallization temperature (T_c) of all samples were inspected by using differential scanning calorimetric (DSC) analysis. Moreover, the crystallization and melting enthalpies were evaluated by studying the differential scanning calorimetry (DSC) thermograms. The DSC thermograms for PET polymer and related bionanocomposites are illustrated in Fig. 6. The results of DSC analysis about the variations in the melting, crystallization, and glass transition temperature of PET by additions of different fillers are reported in Table 3. The glass transition temperature of the PET sample in this study was around 80 °C. An exothermic peak at 149 °C was related to the cold crystallization of PET. Furthermore, an endothermic peak related to the melting temperature for applied PET was observed at about 249 °C. The insertion of these ingredients into the PET matrix caused major variations in the thermal behavior of PET. Therefore, as can be observed, the T_g of PET decreased by 4 °C, reaching 76.1 °C. The T_{cc} value for PET decreased to 123 °C after the insertion of modified chitosan, whereas the T_m value

Fig. 2 FT-IR spectra of the PET and PET nano-composites in the range of 4000–400 cm^{-1}

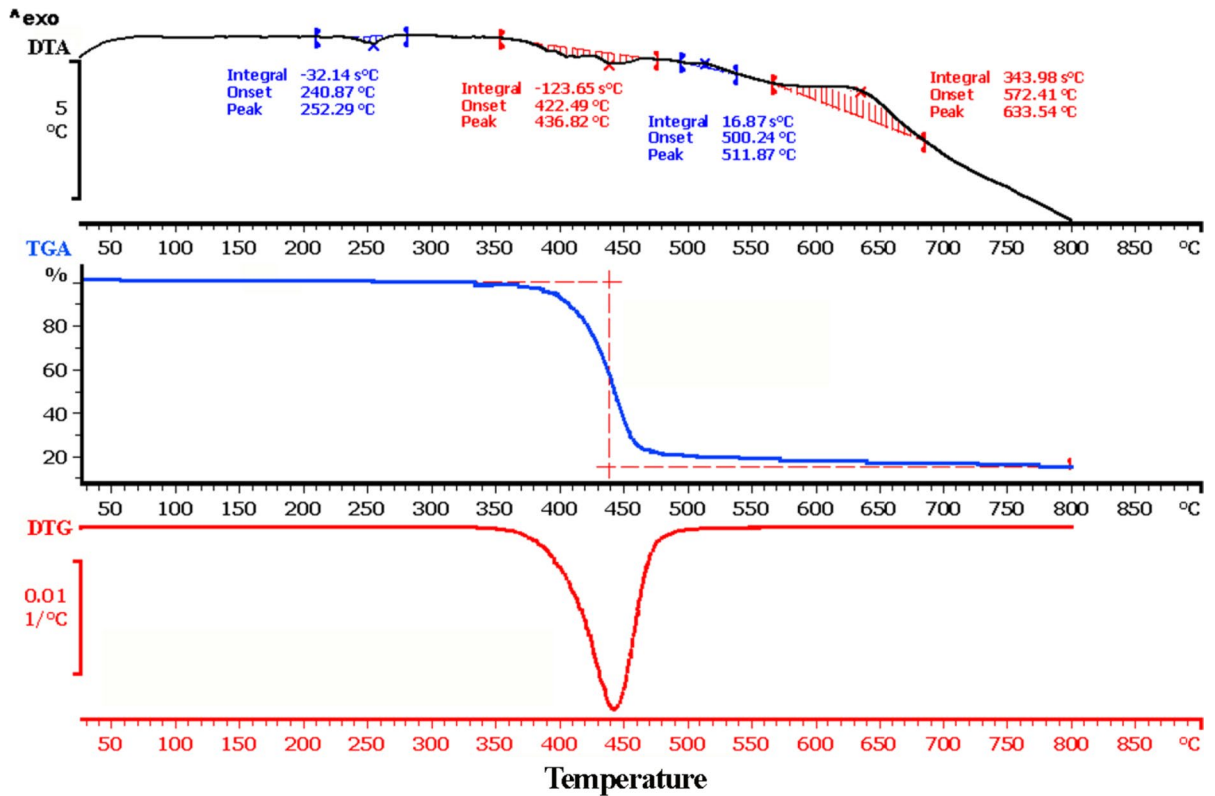
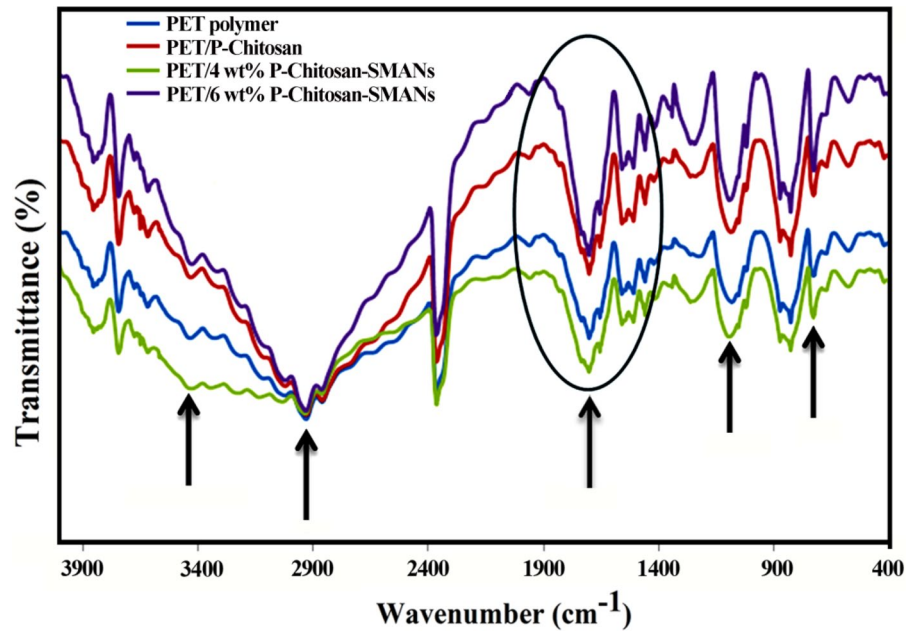


Fig. 3 TGA, DTG and DTA analysis results for PET/P-Chitosan/4 wt%SMANs

Fig. 4 TGA comparative curves of PET and PET nanocomposites

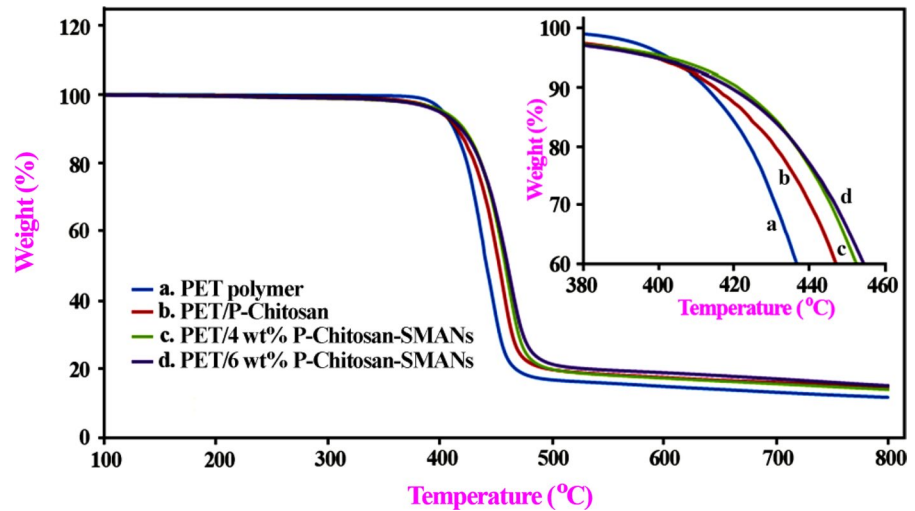
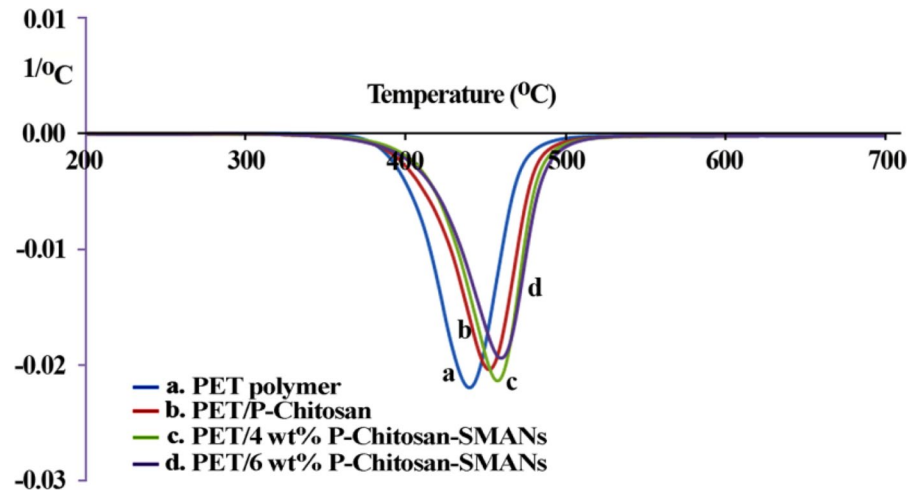


Table 2 TGA results of prepared nanocomposites

Sample	T_{max}^b (°C)	$T_{10\%}^a$ (°C)	Char Yield c (%)	LOI d
PET/P-Chitosan/4 wt%SMANs	418.5	454.6	14.11	23.14
PET/P-Chitosan/6 wt%SMANs	420.8	457.8	15.41	23.68

^aTemperature at which 10% mass loss was recorded by TGA at a heating rate of 10 °C/min under a nitrogen atmosphere. ^bTemperature at which maximum mass loss was recorded by TGA at a heating rate of 10 °C min⁻¹ under a nitrogen atmosphere. ^cWeight percentage of material left undecomposed after TGA analysis at 600 °C. ^dLimiting oxygen index (LOI) evaluating char yield at 600°C.

Fig. 5 DTG curves for PET and PET nanocomposites



decreased to 247.6 °C by the insertion of phosphorylated chitosan. This reduction in the T_g value, as well as the T_{cc} value, was related to the decrease in the molecular weight in the presence of phosphorylated chitosan. This result was confirmed by the viscosity test. The viscosity test results show that the intrinsic

viscosity value for PET was 0.781 dL g⁻¹. By adding phosphorylated chitosan to PET, the intrinsic viscosity value for the PET/phosphorylated chitosan compound changed to 0.420 dL g⁻¹. The presence of phosphorylated chitosan structures between the PET chains reduces the molecular mass and increases the

Fig. 6 DSC thermographs for PET and related nanocomposites

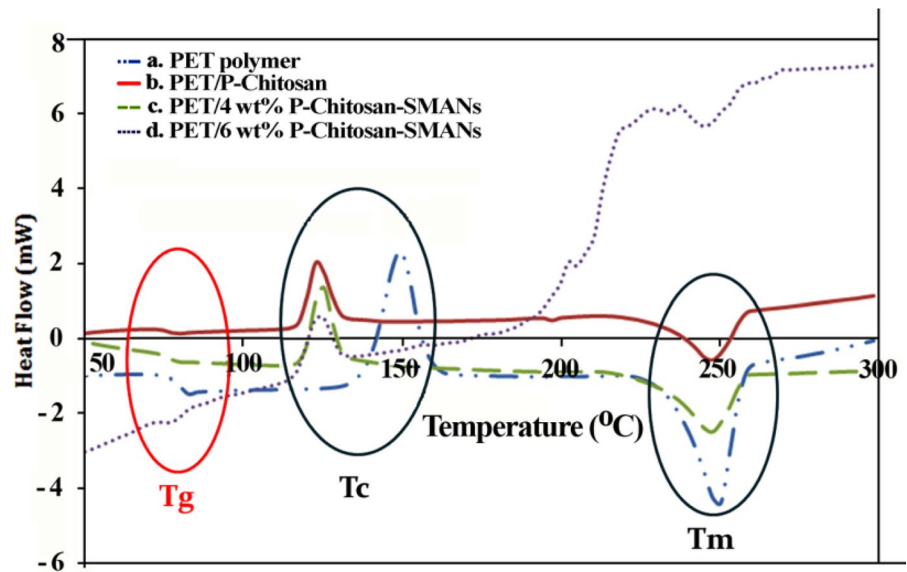


Table 3 DSC analysis results of prepared nanocomposites

Sample	T_g (°C)	T_{cc} (°C)	ΔH_{cc} (J g ⁻¹)	T_m (°C)	ΔH_m (J g ⁻¹)
PET/4 wt% P-Chitosan-SMANs	77.4	124.5	22.6	247.2	36.4
PET/6 wt% P-Chitosan-SMANs	77.8	123.6	19.3	246.2	11.8

freedom of movements of polymer chains. The role of phosphorylated chitosan was related to the nucleating effect and, therefore, based on this concept, the glass transition temperature decreased. Furthermore, the higher degree of freedom, reduced chain length and lesser physical entanglement resulted in an increase in crystallinity values. The PET values of cold crystallization enthalpy (ΔH_{cc}) and melting enthalpy (ΔH_m) changed in the presence of phosphorylated chitosan. These results also support the enhancement in the crystallinity of compounded PET in the presence of phosphorylated chitosan.

The application of nanoscale surface-modified alumina along with phosphorylated chitosan also showed similar trends for values of T_g , T_{cc} , and T_m . The decreasing trend in intrinsic viscosity values was observed for bionanocomposite samples in the presence of phosphorylated chitosan/nano alumina. The intrinsic viscosity values for bionanocomposites containing 4 wt%, and 6 wt% phosphorylated chitosan/modified alumina nanoparticles were 0.392 and 0.384 dL g⁻¹, respectively. As noted from the thermograms, slight increases in the T_g values and increases in the enthalpy of melting values were detected for samples

containing 4 and 6 wt% of PET/phosphorylated chitosan/nano alumina. Some of the interactions of surface-modified alumina nanoparticles supported on the phosphorylated chitosan with PET polymer chains caused an increase in the values of T_g . The increase in the content of phosphorylated chitosan-nano alumina up to 6 wt% was accompanied by a significant decrease in the melting and crystallization enthalpy values. This behavior is evidently due to the nucleating effect favored by the phosphorylated chitosan/nano alumina on PET crystallization and seems to be independent of the filler content, indicating the saturation of the nucleating effect at phosphorylated chitosan/nano alumina contents above 4 wt%. Based on these data, we can deduce that there is enough compounded nanofiller present to provide an adequate surface area. Therefore, the determining step in the overall crystallization process is more strongly related to the crystal growth than to the nucleation process. Normally, the use of phosphorylated chitosan along with surface-modified alumina nanoparticles reduces the PET molecular weight, thereby resulting in a drop in the T_g value, which facilitates the crystallization process.

Morphological characterization of surface-modified nanoparticles, PET and related bionanocomposites by scanning electron microscopy

The scanning electron microscopy (SEM) was used to investigate the morphology of alumina nanostructures, PET polymer, PET/phosphorylated chitosan, and the dispersion of phosphorylated chitosan/surface-modified nano alumina in PET bionanocomposites. The effects of adding phosphorylated chitosan to the microstructures and morphology of prepared compounds were also studied by SEM. SEM micrographs of alumina nanoparticles before (a, and b) and after the surface-modification process are shown in Fig. 7. It appears that, after the modification, the dispersion properties of the nanostructure were improved, and

the agglomerated structure was not detected (c, and d). The SEM micrographs of PET and PET/phosphorylated chitosan are shown in Fig. 8a and b. Due to the compatible nature of chitosan and PET, phosphorylated chitosan was compounded with PET. Figure 8 illustrates that there is complete compatibility between the phosphorylated chitosan and the PET matrix. Neither separated phases, micro-cracks nor holes were detected in the SEM image of the compounded sample (Fig. 8b) related to the chitosan phase. Therefore, the compatibility of phosphorylated chitosan and PET is proven. The morphological characterizations of surface-modified alumina nanoparticles, and combination with phosphorylated chitosan in PET bionanocomposites were observed using SEM. The SEM micrographs of the samples are

Fig. 7 SEM micrographs of alumina nanoparticles before **a** and **b** and after **c** and **d** surface modification

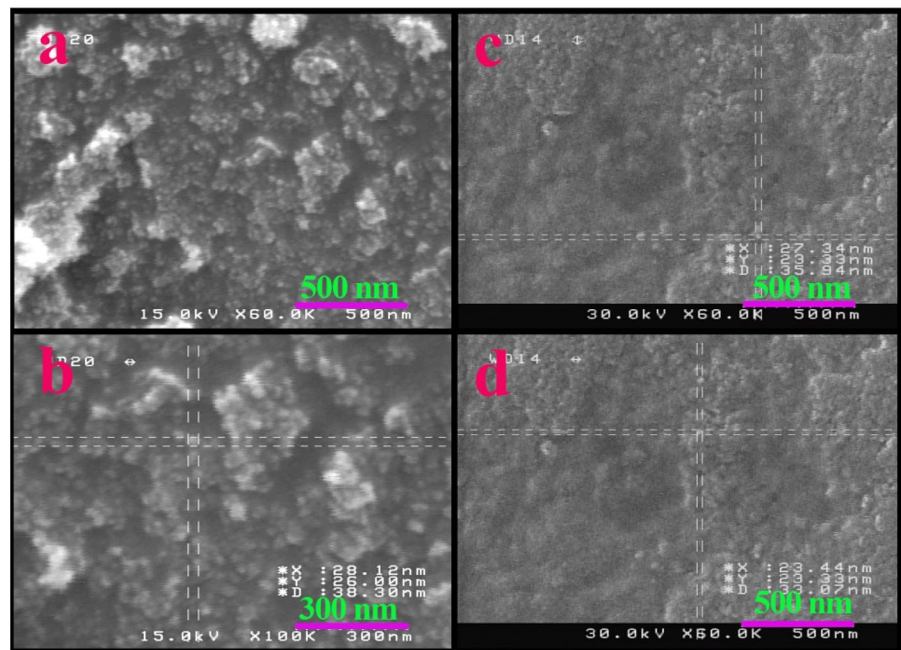
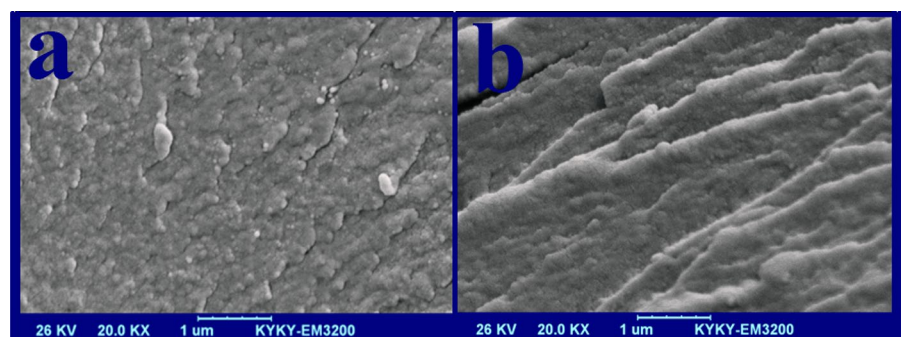


Fig. 8 SEM micrographs of PET **a** and PET/phosphorylated chitosan **b**



shown in Fig. 9. The diameter of the alumina nanoparticles after modification with Leucine amino acid is a little bigger than that of pure alumina; this can be due to the interaction of the amino acid with the surface functional units of the nanostructure. The sizes of alumina nanoparticles in provided nanocomposites are in the range of 50–68 nm. It can be observed that the phosphorylated chitosan/PET has a lamellar structure and a flatter surface morphology than that of the bionanocomposites; moreover, spherical particles were detected for the bionanocomposites. For the nanoscale alumina supported on phosphorylated chitosan in PET bionanocomposites, there was a uniform distribution of nanoscale elements and protruded particles from the PET matrix, and the perceptible aggregation was not distinguished. The SEM micrographs for the provided bionanocomposites at 4 and 6wt%

are illustrated in Fig. 9a–f. SEM micrographs of nano-additives at 4 and 6wt% are shown in Fig. 9a–c and Fig. 9d–f, respectively.

Qualitative tests of PET and its bionanocomposites

PET is an important polymer in industry; therefore, it is common to evaluate the properties of PET by simple qualitative tests, before carrying out more complicated tests. The data obtained by the qualitative tests for pure PET, phosphorylated chitosan/PET and bionanocomposite samples are reported in Table 4. The intrinsic viscosity values of the prepared samples show a decreasing trend. With enhancement in the filler contents, the values of intrinsic viscosity are reduced. Pure PET shows the maximum intrinsic viscosity value. The intrinsic

Fig. 9 SEM micrographs of nanocomposites: **a–c** pictures for PET/4 wt% phosphorylated chitosan/ Al_2O_3 , and **d–f** pictures for PET/6 wt% phosphorylated chitosan/ Al_2O_3 samples

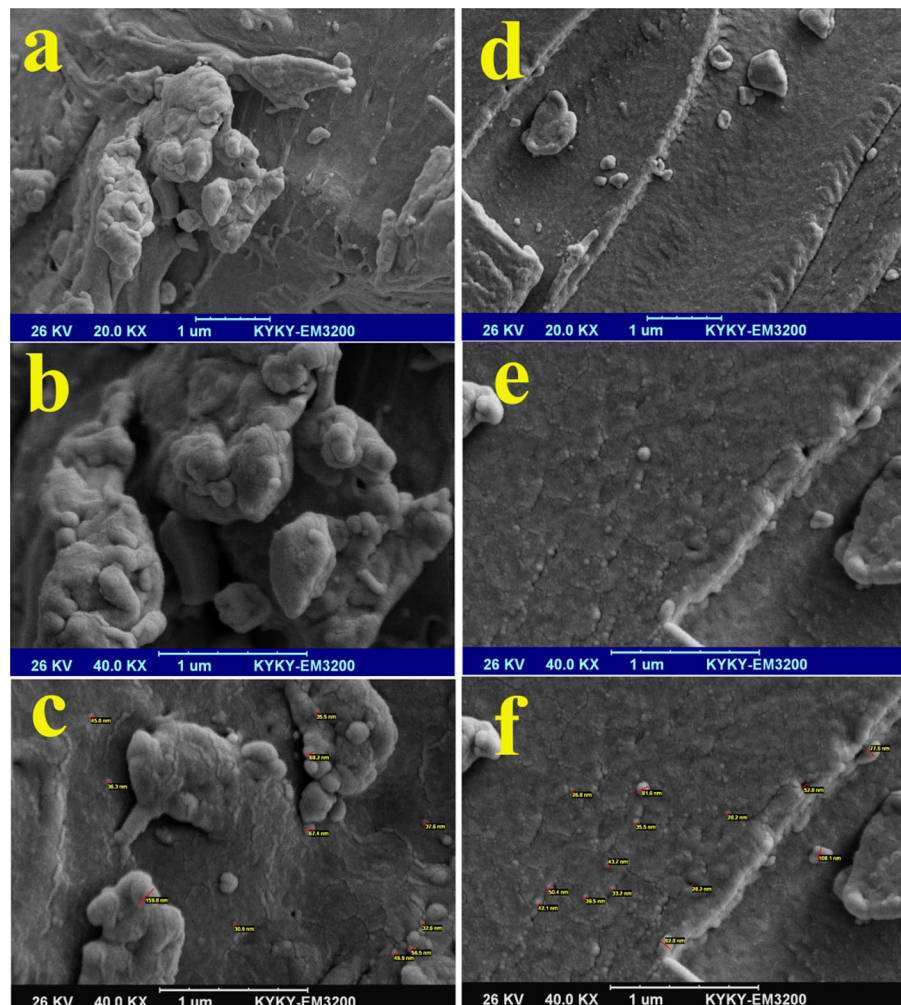


Table 4 Qualitative tests for prepared nanocomposites

Samples	IV (dl/g)	Carboxylic end groups (meq Kg ⁻¹)	Color		
			L*	b*	a*
PET/P-Chitosan/4 wt%SMANs	52	5.5	1.36	9	0.392
PET/P-Chitosan/6 wt%SMANs	98	5.5	2.3	9	0.384

L*: A measure of the brightness and darkness of the product.

b*: A measure of the yellowness and blueness of the product.

a*: A measure of the redness and greenness of the product.

viscosity provides information about the shape, flexibility and molar mass of the polymer structure. The intrinsic viscosity is defined as the reduced specific viscosity in the limit of “infinite dilution” or zero concentration. As was observed in this study, the intrinsic viscosity of PET was reduced by insertion of phosphorylated chitosan and phosphorylated chitosan/nano alumina additives. The reduction in the molecular weight of PET in the presence of phosphorylated chitosan is related to the melt processing and the possibility of hydrolysis of PET chains at high temperature. PET is a polycondensation polymer made of diol and dicarboxylic acid monomers. The experimental results show that the concentration of carboxylic functional units decreases by insertion of modified fillers. This is related to the possible interactions of phosphorylated chitosan chains as well as surface functional units of nanoscale alumina. In the colorimetric measurements, PET fundamentally tended to be yellow; hereafter, the color of the product was adjusted using constituents such as cobalt and blue toner. The cobalt toner contains blue and red pigments, whereas the blue toner contains blue pigment. In this test, each of the parameters L *, b * and a * specifies a certain color range:

L*, b* and a* are the color parameters for the evaluation of the polymer-based products, whose ranges of variation were different. Alumina nanoparticles increased the parameter of a* and, therefore, these nanoparticles tended to create an inappropriate color in the product. The yellowish parameter decreased in the presence of phosphorylated chitosan/alumina nanoparticles. Moreover, the redness of the product decreased by the insertion of the phosphorylated chitosan/alumina nanoparticles. The evaluation of the L* parameter shows that the bionanocomposite containig

6 wt% filler had the same value for L* as the primary PET. This is related to the characteristics of metal oxides that account for the colors of polymers.

Antibacterial assessment of PET and related bionanocomposites

Chitosan is a well-known biopolymer. It has also been reported that chitosan possesses significant antibacterial activity against a wide range of bacteria. In addition, due to the superior surface area of metal oxide nanoparticles, they are expected to behave as antimicrobial agents. Nanoscale alumina has been effectively used against different microorganisms (Poborilova et al. 2013; Pakrashi et al. 2013; Sadiq et al. 2009). Few studies have focused in the evaluation of the toxicity of chitosan in combination with nano alumina against microorganisms. This study analyzes the antibacterial properties of PET polymer, PET/phosphorylated chitosan and PET/phosphorylated chitosan/alumina bionanocomposites with different contents. The bacterial culture test results for polymer sample, intermediate products and final nanocomposites are reported in Table 5. The results show that pure PET can inhibit the growth of bacteria for more than 12 h. The antibacterial activity of the obtained materials was inspected by counting the colonies that formed in the culture medium. The addition of phosphorylated chitosan to PET showed a great improvement in antibacterial activity. Conversely, excessive resistance to bacterial growth was observed for nanocomposites containing 6 wt% phosphorylated chitosan/nano alumina. Typically, after a 12-h bacterial culture test, the bacterial growth in the bionanocomposite sample is over fifteen times that of the initial environment. For long periods (over 20 h), the number of bacteria in the bionanocomposite sample

Table 5 Bacterial culture test results

Experiment media	Experiment time (h)				
	4	8	12	16	20
Culture medium in the presence of <i>E.coli</i>	0.048	0.823	1.24	1.53	1.72
Culture medium in the presence of <i>E.coli</i> and PET	0.033	0.957	1.23	1.205	1.105
Culture medium in the presence of <i>E.coli</i> and 6wt% nanocomposite	0	0.098	0.075	0.205	0.37

is approximately one third of that of the bacteria that grew in the initial environment. These results fully support the antibacterial activity of this bionanocomposite sample.

Conclusions

In this research, PET-based bionanocomposites containing phosphorylated chitosan and alumina nanoparticles were prepared in four steps. A simple, cost-effective, and environmentally friendly sonochemical method along with an internal mixing process was used for the fabrication of bionanocomposites. The change in morphological, thermal and antibacterial properties of PET composites due to the use of phosphorylated chitosan and aluminum nanoparticles were investigated. The thermal properties of PET bionanocomposites were characterized using DSC, TGA, and DTG analyses. The TGA results showed that the initial decomposition temperature of the PET matrix increased by the addition of phosphorylated chitosan. Moreover, the thermal degradation temperature of PET improved with the use of nanoparticles in the presence of phosphorylated chitosan. Therefore, the simultaneous use of phosphorylated chitosan and nano alumina could provide a significant improvement in the thermal stability of PET. The addition of alumina nanoparticles improves bacterial growth inhibition.

Acknowledgments We wish to express our thankfulness to the Research Affairs Division of the Islamic Azad University (Mahshahr branch) and to the University of Bonab (Bonab) for partial financial support. Further financial support from Iran Nanotechnology Initiative Council (INIC) is appreciatively acknowledged. Partial financial support was received from Junta de Extremadura and Fondos Europeos de Desarrollo Regional (GR18035 and GR18171).

Author contributions All authors contributed to the study conception and design. Materials preparations were performed

by AS, RS: data collection and analysis were performed by ND, MQ, FK and NR; MH, HK-M, CJD-V, and IML-C: contributed in writing the first draft of the manuscript and the revised version.

Funding Open Access funding provided thanks to the CRUECSIC agreement with Springer Nature. This study was supported by Iran Nanotechnology Initiative Council, Consejería de Educación y Empleo, Junta de Extremadura, GR21107, GR18171.

Declarations

Conflict of interest The authors declare that they have no competing interests that are relevant to the content of this article.

Open Access This article is licensed under a Creative Commons Attribution 4.0 International License, which permits use, sharing, adaptation, distribution and reproduction in any medium or format, as long as you give appropriate credit to the original author(s) and the source, provide a link to the Creative Commons licence, and indicate if changes were made. The images or other third party material in this article are included in the article's Creative Commons licence, unless indicated otherwise in a credit line to the material. If material is not included in the article's Creative Commons licence and your intended use is not permitted by statutory regulation or exceeds the permitted use, you will need to obtain permission directly from the copyright holder. To view a copy of this licence, visit <http://creativecommons.org/licenses/by/4.0/>.

References

- Ahmadi M, Rad-Moghadam K, Hatami M (2018) From Parkinson's chemotropic agent l-dopa to thermally resistive carbonaceous nanocomposite of a new catecholgrafted poly(amide-imide). *Polymer* 149:1–12. <https://doi.org/10.1016/j.polymer.2018.06.053>
- Al G, Aydemir D, Kaygin B, Ayrilmis N, Gunduz G (2017) Preparation and characterization of biopolymer nanocomposites from cellulose nanofibrils and nanoclays. *J Compos Mater* 52:689–700. <https://doi.org/10.1177/002198317713589>
- Anis A, Elnour AY, Alhamidi A, Alam MA, Saeed MAZ, Alfayez F, Bashir Z (2022) Amorphous poly(ethylene

- terephthalate) composites with high-aspect ratio aluminum nano platelets. *Polymers* 14(3):630. <https://doi.org/10.3390/polym14030630>
- Aoyama S, Ismail I, Park YT, Yoshida Y, Macosko CW, Ougizawa T (2018) Polyethylene terephthalate/trimellitic anhydride modified graphene nanocomposites. *ACS Appl Nano Mater* 1(11):6301–6311. <https://doi.org/10.1021/acsnm.8b01525>
- Babaahmadi V, Abuzade RA, Montazer M (2022) Enhanced ultraviolet-protective textiles based on reduced graphene oxide-silver nanocomposites on polyethylene terephthalate using ultrasonic-assisted in-situ thermal synthesis. *J Appl Polym Sci* 139(21):52196. <https://doi.org/10.1002/app.52196>
- Bahramian A (2021) Poly(ethylene terephthalate)-based nanocomposite films as greenhouse covering material: environmental sustainability, mechanical durability, and thermal stability. *J Appl Polym Sci* 138(10):49991. <https://doi.org/10.1002/app.49991>
- Barber NA (2017) Polyethylene terephthalate: uses, properties and degradation, Nova Science publishers ISBN: 978–153612014–1, 978–153611991–6
- Bezerra RM, Monteiro RRC, Andrade Neto DM, da Silva FFM, de Paula RCM, de Lemos TLG, Fachine PBA, Correa MA, Bohn F, Gonçalves LRB, dos Santos JCS (2020) A new heterofunctional support for enzyme immobilization: PEI functionalized Fe₃O₄ MNPs activated with divinyl sulfone. Application in the immobilization of lipase from *Thermomyces lanuginosus*. *Enzyme Microb Technol* 138:109560. <https://doi.org/10.1016/j.enzmictec.2020.109560>
- Chaudhary P, Fatima F, Kumar A (2020) Relevance of nanomaterials in food packaging and its advanced future prospects. *J Inorg Organomet Polym* 30:5180–5192. <https://doi.org/10.1007/s10904-020-01674-8>
- Chen X, Li C, Shao W, Liu T, Wang L (2008) Nonisothermal crystallization kinetics of poly(ethylene terephthalate)/antimony-doped tin oxide nanocomposites. *J Appl Polym Sci* 109(6):3753–3762. <https://doi.org/10.1002/app.28069>
- De Filipo G, Nicoletta FP, Chidichimo G (2006) Flexible nanophoto-electrochromic film. *Chem Mater* 18:4662–4666. <https://doi.org/10.1021/cm061438m>
- De Guzman MR, Wen YH, Du J, Yuan L, Wu CS, Hung WS, Guo JP, Yao YL, Yuan S, Wang RY, Suen MC, Tsou CH (2021) Characterization of antibacterial nanocomposites of polyethylene terephthalate filled with nanosilver-doped carbon black. *Polym Polym Compos* 29:797–806. <https://doi.org/10.1177/0967391120935305>
- De Moura MR, Mattoso LHC, Zucolotto V (2012) Development of cellulose-based bactericidal nanocomposites containing silver nanoparticles and their use as active food packaging. *J Food Eng* 109:520–524. <https://doi.org/10.1016/j.jfoodeng.2011.10.030>
- de Oliveira UMF, Lima de Matos LJB, de Souza MCM, Pinheiro BB, dos Santos JCS, Gonçalves LRB (2019) Efficient biotechnological synthesis of flavor esters using a low-cost biocatalyst with immobilized *Rhizomucor miehei* lipase. *Mol Biol Rep* 46:597–608. <https://doi.org/10.1007/s11033-018-4514-z>
- Dos Santos JCS, Garcia-Galan C, Rodrigues RC, Batistade Sant'Ana H, Gonçalves LRB, Fernandez-Lafuente R (2014) Stabilizing hyperactivated lecitase structures through physical treatment with ionic polymers. *Process Biochem* 49(9):1511–1515. <https://doi.org/10.1016/j.procbio.2014.05.009>
- Dubrovsky VV, Shapovalov VA, Aderikha VN, Pesetskii SS (2018) Effect of hybrid filling with short glass fibers and expanded graphite on structure, rheological and mechanical properties of poly(ethylene terephthalate). *Mater Today Commun* 17:15–23. <https://doi.org/10.1016/j.mtcomm.2018.08.002>
- Dufresne A, Thomas S, Pothien LA (2013) Biopolymer nanocomposites: processing, properties, and applications Wiley ISBN: 978–1–118–21835–8
- Fidanovski BZ, Popovic IG, Radojevic VJ, Radisavljevic IZ, Perisic SD, Spasojevic PM (2018) Composite materials from fully bio-based thermosetting resins and recycled waste poly(ethylene terephthalate). *Compos B Eng* 153:117–123. <https://doi.org/10.1016/j.compositesb.2018.07.034>
- Ghanbari N, Gharufi H (2002) Design and preparation the novel polymeric layered double hydroxide nanocomposite (LDH/Polymer) as an efficient and recyclable adsorbent for the removal of methylene blue dye from water. *Environ Technol Innov* 26:102377. <https://doi.org/10.1016/j.eti.2022.102377>
- Guerra MA, Swerts JP, Funcia MA, Mariano NA, Campos MGN (2018) Characterization of pet-silver nanocomposite filaments. *Mater Sci Forum* 930:224–229. <https://doi.org/10.4028/www.scientific.net/MSF.930.224>
- Hassan TA, Rangari VK, Jeelani S (2014) Value-added biopolymer nanocomposites from waste eggshell-based CaCO₃ nanoparticles as fillers. *ACS Sustain Chem Eng* 2:706–717. <https://doi.org/10.1021/sc400405v>
- Hatami M (2017) Production and morphological characterization of low resistance polyimide/silver nanowire nanocomposites: potential application in nanoconductive adhesives. *J Mater Sci Mater Electron* 28:3897–3908. <https://doi.org/10.1007/s10854-016-6003-2>
- Hatami M (2018) Production of polyimide ceria nanocomposites by development of molecular hook technology in nano-sonochemistry. *Ultrason Sonochem* 44:261–271. <https://doi.org/10.1016/j.ultsonch.2018.02.032>
- Hatami M, Yazdan Panah M (2017) Ultrasonic assisted synthesis of nanocomposite materials based on resole resin and surface modified nano CeO₂: chemical and morphological aspects. *Ultrason Sonochem* 39:160–173. <https://doi.org/10.1016/j.ultsonch.2017.04.028>
- Hatami M, Azarkar BF, Qandalee M, Hasanabadi H (2015) Morphological investigation of synthetic poly(amic acid)/cerium oxide nanostructures. *Polym Eng Sci* 55:2339–2348. <https://doi.org/10.1002/pen.24122>
- Hatami M, Ahmadipour M, Asghari S (2017) Heterocyclic grafting functionalization of silica nanoparticles: fabrication, morphological investigation and application for PVA nanocomposites. *J Inorg Organomet Polym* 27:1072–1083. <https://doi.org/10.1007/s10904-017-0557-1>
- Hatami M, Yazdan Panah M, Mahmoudian M (2020) Facile production of HNTs/VPDAPF nanocomposites by unique and environment-friendly method for the removal of phenolic pollutants in water as an environmental adsorbent.

- J Taiwan Inst Chem Eng 108:1–15. <https://doi.org/10.1016/j.jtice.2020.01.001>
- Hatami M, Sharifi A, Karimi-Maleh H, Agheli H, Karaman C (2022) Simultaneous improvements in antibacterial and flame retardant properties of PET by use of bio-nanotechnology for fabrication of high performance PET bionanocomposites. *Environ Res* 206:112281. <https://doi.org/10.1016/j.envres.2021.112281>
- <https://www.byk.com>, accessed 1-may-2022
- <https://www.nyacol.com/>, accessed 1-may-2022
- Jalali SAH, Allafchian A, Bahramian H, Amiri R (2017) An antibacterial study of a new magnetite silver nanocomposite. *J Environ Chem Eng* 5:5786–5792. <https://doi.org/10.1016/j.jece.2017.11.016>
- Jia J, Gai Y, Wang W, Zhao Y (2016) Green synthesis of biocompatible chitosan-graphene oxide hybrid nanosheet by ultrasonication method. *Ultrason Sonochem* 32:300–306. <https://doi.org/10.1016/j.ultsonch.2016.03.027>
- Joo S, Cho JJ, Seo H, Son HF, Sagong HY, Shin TJ, Choi SY, Lee SY, Kim KJ (2018) Structural insight into molecular mechanism of poly(ethylene terephthalate) degradation. *Nat Commun* 9:382. <https://doi.org/10.1038/s41467-018-02881-1>
- Jothimani B, Sureshkumar S, Venkatachalapathy B (2017) Hydrophobic structural modification of chitosan and its impact on nanoparticle synthesis – a physicochemical study. *Carbohydr Polym* 173:714–720. <https://doi.org/10.1016/j.carbpol.2017.06.041>
- Jung DE, Hahm WG, Kikutani T, Kim BC (2018) Structural factor of nanoparticles in the stress-induced crystallization of poly(ethylene terephthalate). *Compos Sci Technol* 165:314–321. <https://doi.org/10.1016/j.compscitech.2018.07.020>
- Khoe S, Saadatinia A, Bafkary R (2017) Ultrasound-assisted synthesis of pH-responsive nanovector based on PEG/chitosan coated magnetite nanoparticles for 5-FU delivery. *Ultrason Sonochem* 39:144–152. <https://doi.org/10.1016/j.ultsonch.2017.04.025>
- Lim SK, Choi WM, Choi HJ, Hong SH, Hwang SH, Kim S, Lee SH, Kim KW (2013) Synthesis and characterization of poly(ethylene terephthalate)/Al₂O₃ nanocomposites. *Adv Mater Res* 717:54–57. <https://doi.org/10.4028/www.scientific.net/AMR.717.54>
- Lima JC, Costa ARM, Sousa JC, Arruda SA, Almeida YMB (2021) Thermal behavior of polyethylene terephthalate/organoclay nanocomposites: investigating copolymers as matrices. *Polym Compos* 42(2):849–864. <https://doi.org/10.1002/pc.25870>
- Liu W, Tian X, Cui P, Li Y, Zheng K, Yang Y (2004) Preparation and characterization of PET/Silica Nanocomposites 91(2) 1229–1232 <https://doi.org/10.1002/app.13284>
- Madakbas S, Türk Z, Sen F, Vezir Kahraman M (2017) Thermal and morphological properties of organo modified nanoclay/polyethylene terephthalate composites. *J Inorg Organomet Polym* 27:31–36. <https://doi.org/10.1007/s10904-016-0438-z>
- Mallakpour S, Motirasoul F (2017) Use of PVA/ α -MnO₂-stearic acid nanocomposite films prepared by sonochemical method as a potential sorbent for adsorption of Cd (II) ion from aqueous solution. *Ultrason Sonochem* 37:623–633. <https://doi.org/10.1016/j.ultsonch.2017.02.025>
- Mehdipour-Ataei S, Hatami M (2007) Aromatic poly(sulfone sulfide amide)s as new types of soluble thermally stable polymers. *Polym Adv Technol* 18:292–298. <https://doi.org/10.1002/pat.864>
- Mehdipour-Ataei S, Sarrafi Y, Hatami M (2005) Naphthalene-ring containing diamine and resulting thermally stable polyamides. *Eur Polym J* 41(12):2887–2892. <https://doi.org/10.1016/j.eurpolymj.2005.06.012>
- Mehdipour-Ataei S, Hatami M, Mosslemin MH (2009) Organosoluble, thermally stable polyamides containing sulfone and sulfide units. *Chin J Polym Sci* 27(6):781–787. <https://doi.org/10.1142/S0256767909004497>
- Melo ADQ, Silva FFM, Dos Santos JCS, Fernández-Lafuente R, Lemos TLG, Dias Filho FA (2017) Synthesis of benzyl acetate catalyzed by lipase immobilized in nontoxic chitosan-polyphosphate beads. *Molecules* 22(12):2165. <https://doi.org/10.3390/molecules22122165>
- Monteiro RRC, Lima PJM, Pinheiro BB, Freire TM, Dutra LMU, Fechine PBA, Gonçalves LRB, de Souza MCM, Dos Santos JCS, Fernández-Lafuente R (2019) Immobilization of lipase a from *Candida antarctica* onto chitosan-coated magnetic nanoparticles. *Int J Mol Sci* 20(16):4018. <https://doi.org/10.3390/ijms20164018>
- Naffakh M, Marco C, Ellis G (2014) Development of novel melt-processable biopolymer nanocomposites based on poly(L-lactic acid) and WS2 inorganic nanotubes. *Cryst-EngComm* 16(23):5062–5072. <https://doi.org/10.1039/c3ce42593b>
- Ou CF, Ho MT, Lin JR (2004) Synthesis and characterization of poly(ethylene terephthalate) nanocomposites with organoclay. *J Appl Polym Sci* 91(1):140–145. <https://doi.org/10.1002/app.13158>
- Pakrashi S, Dalai S, TC P, Trivedi S, Myneni R, Raichur AM, Chandrasekaran N, Mukherjee A (2013) Cytotoxicity of aluminium oxide nanoparticles towards fresh water algal isolate at low exposure concentrations. *Aquatic Toxicol* 132–133, 34–45 <https://doi.org/10.1016/j.aquatox.2013.01.018>
- Peng X, Ding E, Xue F (2012) In situ synthesis of TiO₂/polyethylene terephthalate hybrid nanocomposites at low temperature. *Appl Surf Sci* 258(17):6564–6570. <https://doi.org/10.1016/j.apsusc.2012.03.077>
- Phung Hai TA, Sugimoto HR (2018) Surface modification of chitin and chitosan with poly(3-hexylthiophene) via oxidative polymerization. *Appl Surf Sci* 434:188–197. <https://doi.org/10.1016/j.apsusc.2017.10.197>
- Poborilova Z, Opatrilova R, Babula P (2013) Toxicity of aluminium oxide nanoparticles demonstrated using a BY-2 plant cell suspension culture model. *Environ Exp Bot* 91:1–11. <https://doi.org/10.1016/j.envexpbot.2013.03.002>
- Rathod VT, Kumar JS, Jain A (2017) Polymer and ceramic nanocomposites for aerospace applications. *Appl Nanosci* 7:519–548. <https://doi.org/10.1007/s13204-017-0592-9>
- Rodriguez SA, Weese E, Nakamatsu J, Torres F (2016) Development of biopolymer nanocomposites based on polysaccharides obtained from red algae chondracanthus chamissoi reinforced with chitin whiskers and montmorillonite. *Polym Plast Technol Eng* 55(15):1557–1564. <https://doi.org/10.1080/03602559.2016.1163583>
- Sadhasivam B, Rigana MF, Rukmanikrishnan B, Muthusamy S (2018) Chiral polyimide and its nanocomposites with graphene oxide using l-phenylalanine-based diamine.

- Polym Bull 75(2):829–849. <https://doi.org/10.1007/s00289-017-2050-y>
- Sadiq IM, Chowdhury B, Chandrasekaran N, Mukherjee A (2009) Antimicrobial sensitivity of *Escherichia coli* to alumina nanoparticles. *Nanomed Nanotechnol* 5(3):282–286. <https://doi.org/10.1016/j.nano.2009.01.002>
- Scheirs J, Long TE (2004) *Modern polyesters: chemistry and technology of polyesters and copolyesters* Wiley <https://doi.org/10.1002/0470090685>
- Siva V, Murugan A, Shameem A, Thangarasu S, Asath Bahadur S (2022) A facile microwave-assisted combustion synthesis of NiCoFe₂O₄ anchored polymer nanocomposites as an efficient electrode material for asymmetric supercapacitor application. *J Energy Storage* 48:103965. <https://doi.org/10.1016/j.est.2022.103965>
- Subashini K, Prakash S, Sujatha V (2022) Biological applications of green synthesized zinc oxide and nickel oxide nanoparticles mediated poly(glutaric acid-co-ethylene glycol-co-acrylic acid) polymer nanocomposites. *Inorg Chem Commun* 139:109314. <https://doi.org/10.1016/j.inoche.2022.109314>
- Van Krevelen DW, Hoftyzer PJ (1976) *Properties of polymers*, 3rd edn. Elsevier
- Visakh PM, Liang M (2015) *Poly(ethylene terephthalate) based blends, composites and nanocomposites*, Elsevier <https://doi.org/10.1016/C2013-0-19172-6>
- Wang K, Zhang W, Guan X, Liu Y, Wei T, Guo W (2018) Fabrication of PET/BiOI/SnO₂ heterostructure nanocomposites for enhanced visible-light photocatalytic activity. *Solid State Sci* 82:34–43. <https://doi.org/10.1016/j.solidstatesciences.2018.05.013>
- Yin XH, Yang C, Tang Y (2019) Multi-scale simulation revealing low thermal conductivity origins of melt-compounded HDPE/MWCNTs nanocomposites. *Int J Therm Sci* 139:350–361. <https://doi.org/10.1016/j.ijthermalsci.2019.02.018>
- Yousefi AR, Savadkoobi B, Zahedi Y, Hatami M, Ako K (2019) Fabrication and characterization of hybrid sodium montmorillonite/TiO₂ reinforced cross-linked wheat starch-based nanocomposites. *Int J Biol Macromol* 131:253–263. <https://doi.org/10.1016/j.ijbiomac.2019.03.083>
- Zhang K, Mao Z, Huang Y, Xu Y, Huang C, Guo Y, Ren X, Liu C (2020) Ultrasonic assisted water-in-oil emulsions encapsulating macro-molecular polysaccharide chitosan: Influence of molecular properties, emulsion viscosity and their stability. *Ultrason Sonochem* 64:105018. <https://doi.org/10.1016/j.ultsonch.2020.105018>

Publisher's Note Springer Nature remains neutral with regard to jurisdictional claims in published maps and institutional affiliations.